

RSC Advances



This is an *Accepted Manuscript*, which has been through the Royal Society of Chemistry peer review process and has been accepted for publication.

Accepted Manuscripts are published online shortly after acceptance, before technical editing, formatting and proof reading. Using this free service, authors can make their results available to the community, in citable form, before we publish the edited article. This *Accepted Manuscript* will be replaced by the edited, formatted and paginated article as soon as this is available.

You can find more information about *Accepted Manuscripts* in the [Information for Authors](#).

Please note that technical editing may introduce minor changes to the text and/or graphics, which may alter content. The journal's standard [Terms & Conditions](#) and the [Ethical guidelines](#) still apply. In no event shall the Royal Society of Chemistry be held responsible for any errors or omissions in this *Accepted Manuscript* or any consequences arising from the use of any information it contains.

COMMUNICATION

A microfluidic process for on-chip formation of assemblies of oxide nanoparticles

Cite this: DOI: 10.1039/x0xx00000x

V. K. Parashar, J. B. Wacker, D. Necula, and M. A. M. Gijs

Received 00th June 2014,

Accepted 00th July 2014

DOI: 10.1039/x0xx00000x

www.rsc.org/advances

We report the continuous growth of spherical assemblies of silica and titania nanoparticles, which were pre-activated to produce hydroxyl/peroxy groups on their surface, by flowing a colloid-in-dioctyl phthalate emulsion into a polydimethylsiloxane microfluidic chip, which is held at a temperature of 120-130 °C. When the colloidal microdroplets enter the chip, the instantaneous heating results in vapour-based convective agitation and emulsion breakup, leading to microdroplet fusion and subsequent merging of their nanoparticle content. This progressively results in a robust large assembly obtained after sintering at 600 °C owing to strong chemical interparticle bonds.

Self-assembly of nanoparticles, in particular three-dimensional (3D) or spherical assemblies^[1-3], is characterized by a high number of interfaces and high specific binding area, which is key for advanced optical^[3-6] or chemical functionality^[7-12]. So far, spherical assembly of colloidal nanoparticles was based on agglomeration of nanoparticles contained in a single droplet upon evaporation of the colloidal fluid^[1, 3, 13-15]. The droplet size and nanoparticle concentration hereby dictated the final size of the assembled object. However, higher oxide concentrations or heavier nanoparticles can result in sedimentation problems and present the limiting factors for the formation of large assemblies starting from a colloidal droplet^[14, 16]. Large silica nanoparticle assemblies were recently prepared by immersing a millimetre-size aqueous colloidal droplet in a very large stirred hot oil bath. In this process, the droplet remained in the oil medium in a spherical state until all water was evaporated, leaving behind a spherical assembly^[17]. We have established a microfluidic droplet process to prepare silica spherical and cylindrical assemblies^[18]. However, a continuous growth of the assembly in a microfluidic process, where nanoparticles form and subsequently join the main spherical assembly in an incremental way, has not been established so far.

Here, we report a process, in which multiple aqueous microdroplets loaded with oxide nanoparticles in a colloid-in-dioctyl phthalate (DOP) emulsion flow at a constant flow rate in a microfluidic chip, held at a temperature of 120-130 °C. At

this temperature, exponentially decrease in DOP viscosity and vaporization of water facilitate emulsion breakup, convective agitation and subsequent merging of all microdroplets that enter the chip over time. Simultaneously, the pre-activated nanoparticles inside the droplets progressively joined layer by layer to form a single large spherical assembly. Using pre-activated nanoparticle surfaces, strong oxide bonds between the nanoparticles are obtained when the assembly is consolidated during a final sintering step at 600 °C.

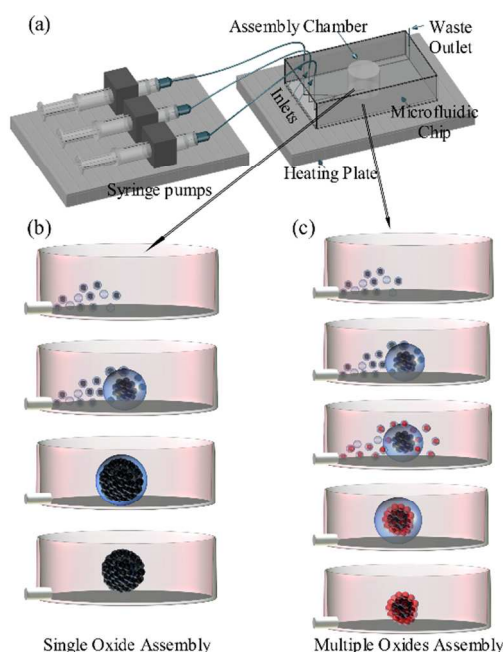


Fig. 1 Schematic of the setup and process used for the formation of nanoparticle assemblies. (a) Microfluidic chip setup; (b) single oxide assembly formation, showing progressive merging of microdroplets and their nanoparticle content into a single spherical assembly; (c) simultaneously flowing of different oxide emulsions results in a multiple oxides spherical assembly.

A schematic of the setup used for the nanoparticle assembly is shown in Fig. 1(a). The reactor part of the chip is a cylindrical

chamber with a height of 6 mm and a diameter of 8 mm. Liquid is fed to the chamber via a microfluidic channel with a width of 160 μm and a height of 40 μm and positioned at the bottom level of the chamber; upstream of this channel are three inlet channels to the chip. The emulsion flow rate and liquid volume that takes part in the process are controlled with a neMESYS syringe pump unit (Cetoni, Korbussen, Germany); one syringe serves to pre-fill the chamber with DOP, one is filled with a silica colloid-in-DOP emulsion, and one with a titania colloid-in-DOP emulsion. Separate inlets for each emulsion provide the flexibility to manipulate the silica to titania ratio in mixed oxide assemblies as well as the possibility to obtain core-shell oxide assemblies. The microfluidic chip is mounted on a mini-heating plate with temperature control. On applying the emulsion into the pre-heated microfluidic chip-chamber at a temperature of 120-130 $^{\circ}\text{C}$, the viscosity of the DOP decreases exponentially and the aqueous microdroplets expand to vapor bubbles. Buoyancy drives the vapour droplets upwards, while gravity brings the nanoparticles back to the bottom of the chamber in a convective agitated flow pattern of the emulsion. During the process, microdroplets increasingly collide and merge. The process continues until emulsion flow to the chip stopped. Thus, forming a single sphere. The final size of the assembly is simply controlled by the number of nanoparticles entered in the chip as aqueous dispersed phase of the emulsion. Fig. 1(b) schematically shows that, upon merging of microdroplets, a small-size spherical assembly is initially generated within the chamber. More incoming microdroplets merge further to build up the assembly in a continuous manner. Fig. 1(c) shows that, using the same process, simultaneous flow of different oxide emulsions permits to form a multiple oxides spherical assembly. The process is controlled by the flow rate, oxide concentration in the colloid and microfluidic chamber dimensions. Our micro-emulsions have 15 vol % aqueous dispersed phase (the process works in the 5-15 vol. % range) in DOP oil medium and TX-100 (1 vol. % in DOP) as surfactant; we used colloidal concentrations of 10 and 25 wt.% oxide in water. Use of higher oxide content makes droplets heavier and results in sedimentation and clogging of the microchannels.

Fig. 2 shows the effect of flow rate and oxide concentration on the size and shape of the assemblies. Fig. 2(a,c,e) are Scanning Electron Microscopy (SEM) photographs of the assemblies obtained after 90 sec of emulsion flow at various flow rates for an emulsion having 10 wt% oxide concentration. Fig. 2(a), obtained for the lowest flow rate of 15 nL/sec, shows agglomerates of a few nanoparticles only, as the supply of the colloid is too low to supply sufficient water vapour, so that thermal agitation is not important enough for formation of a single droplet containing all nanoparticles. However, spherical assemblies are formed at 50 nL/sec flow rate, as shown in Fig. 2(c). Fig. 2(e) shows formation of non-spherical objects at a 100 nL/sec flow rate: a too big water droplet forms at the bottom of the chamber and the nanoparticles tend to sediment to the bottom of it, leaving behind a distorted assembly after water evaporation. Fig. 2(b,d,f) show SEM photographs of assemblies prepared using the same flow rates, but with a more concentrated 25 wt% oxide content of nanoparticles in the emulsion. We found that the 3D assemblies obtained at a flow rate 50 nL/sec are even bigger than before and also well-formed. Fig. S1 of the Electronic Supporting Information (ESI) demonstrates the influence of the size of the microfluidic chamber on the assembly formation, showing an optimum chamber diameter of 8 mm. smaller chamber diameters resulted in an effect of the chamber wall on the big droplet formation

and gave deformed assemblies. Larger chambers resulted in multiple convective patterns and hence multiple assemblies.

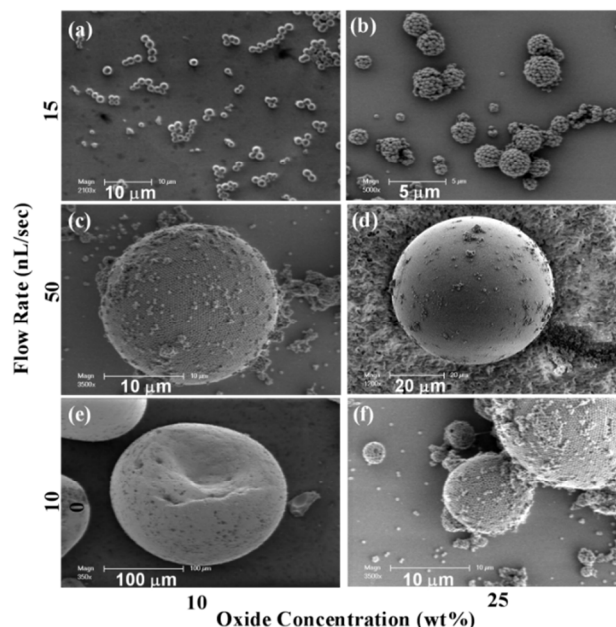


Fig. 2 Effect of flow rate and oxide concentration on the formation of silica nanoparticle assemblies. SEM photographs of the assemblies obtained after 90 sec. at flow rates of (a,b) 15 nL/sec, (c,d) 50 nL/sec and (e,f) 100 nL/sec for emulsions having (a,c,e) 10 wt% oxide concentration and (b,d,f) 25 wt% oxide content of nanoparticles in the emulsion, respectively.

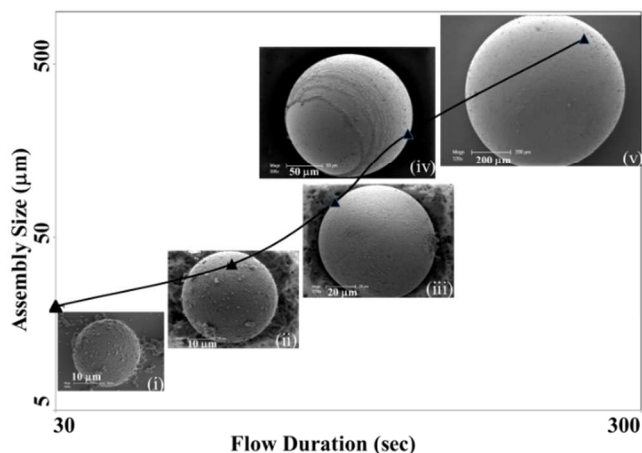


Fig. 3 Effect of flow duration on assembly size. Assemblies are obtained from an emulsion having 15 vol. % aqueous dispersed phase in DOP and 25 wt.% silica in water at a flow rate of 50 nL/sec in a microfluidic chamber of 8 mm diameter and 6 mm height. Assemblies are obtained at different times after initiation of the flow: (i) 30-35 sec, (ii) 60 sec, (iii) 90 sec, (iv) 120 sec, and (v) 240 sec.

Fig. 3 shows SEM photographs of assemblies of silica nanoparticles obtained for different durations of the microfluidic flow, taking a 25 wt% oxide content in a 8 mm diameter chamber: (i) 30-35 sec, (ii) 60 sec, (iii) 90 sec, (iv) 120 sec, and (v) 240 sec. Progressively larger spherical assemblies are formed, as more oxide material is provided for the longer process durations. When the process takes less than 60 sec, the same assemblies are consistently formed, but we noticed the formation of multiplet spherical assemblies and,

associated with it, a higher uncertainty in size for the longer flows.

Demonstrating the wider applicability of the approach, Fig. 4(a,b,c) are SEM photographs of a titania nanoparticle assembly, a hybrid titania-silica assembly, and a magnified picture of a hybrid silica-titania assembly, indicating that our process is suitable for higher specific weight oxides too. Silica colloid-in-DOP and titania colloid-in-DOP emulsions, both having 25 wt% oxide content, were simultaneously pumped into the microfluidic chamber at a flow rate of 50 nL/sec and 15 nL/sec respectively. The bigger size nanoparticles (~360 nm) in Fig. 4(c) are made of silica, and the smaller ones (~150 nm) of titania. Fig. 4(d) is an Energy Dispersive X-ray (EDX)-SEM analysis of the mixed assembly and provides a distribution of silica and titania, corresponding to a weight ratio of ~3:1, in agreement with the colloidal content of the applied flows during the assembly process.

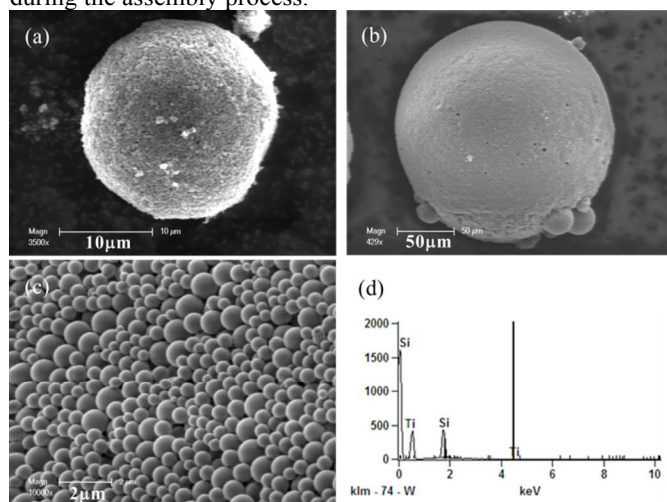


Fig. 4 Demonstration of the wider applicability of our process by forming single and multiple oxides assemblies. SEM photographs of: (a) a titania nanoparticle assembly, (b) a hybrid titania-silica nanoparticle assembly, and (c) a magnified picture of the silica-titania nanoparticle assembly; (d) Energy Dispersive X-ray (EDX) spectrum of the hybrid assembly.

Using native nanoparticles in the colloidal phase of the emulsion inevitably leads to a decomposition of the spherical assembly after drying, because no strong bonds are formed between the inert nanoparticle surfaces. Therefore, an essential requirement for consolidation and permanent joining of the assembly is to pre-activate the surface of the nanoparticles prior to their application into the emulsion. Pre-activation is obtained by hydrothermal treatment of the native nanoparticles to produce hydroxyl and peroxy groups on the silica and titania surface, respectively. Fig. S2 of the ESI shows how activation leads to interparticle joining, when using a sintering step at 600 °C after assembly formation.

Conclusions

We have presented an original microfluidic process for the rapid assembly of oxide nanoparticles into three-dimensional spheres through thermal agitation of a colloid-in-DOP emulsion in a continuous flow microfluidic chip. Use of pre-activated nanoparticles in the dispersed aqueous phase of the emulsion resulted in strong oxide-linked nanoparticles in the consolidated sintered sphere. We expect that these assemblies can be used in many chemical environments for a broad class of applications.

For example, they can offer interesting photonic properties or can be applied in combinatorial chemistry, catalysis, high-throughput screening, multiplex chemical sensing, drug delivery, proton transportation in hydrogen cells, etc.^[1, 2, 4-8, 11, 12, 19]

Acknowledgements. The authors acknowledge the Swiss National Science Foundation for financial support (Grants No. 200020-119788 and 200021-146237).

Notes and references

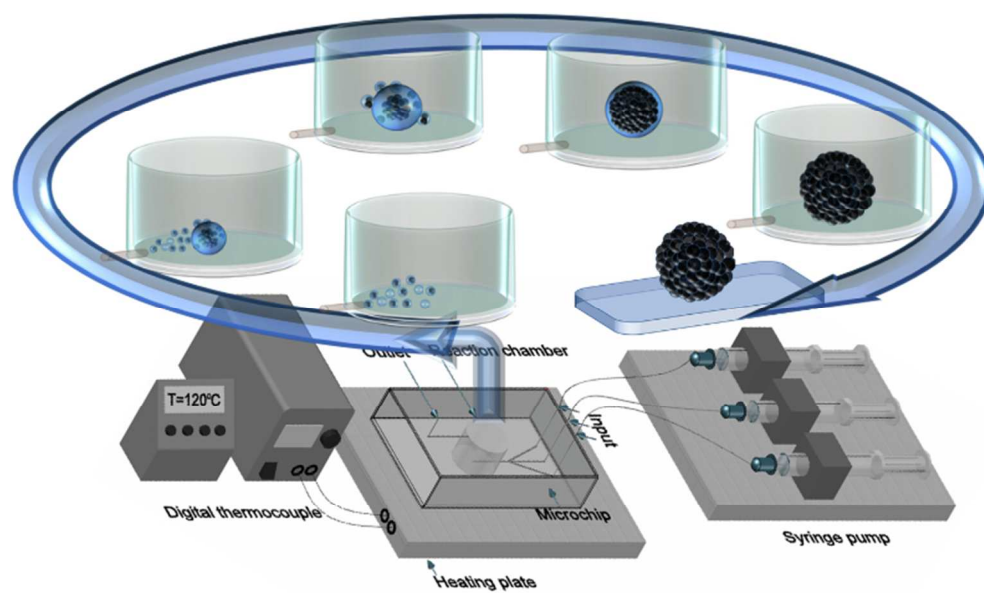
Laboratory of Microsystems, Ecole Polytechnique Fédérale de Lausanne (EPFL), CH-1015 Lausanne, Switzerland

Electronic Supplementary Information (ESI) available: [Experimental section containing: (i) preparation and activation of silica nanoparticles, (ii) preparation and activation of titania nanoparticles, (iii) preparation of emulsions, (iv) fabrication of microfluidic chips. Fig. S1 is on the size effect of the microfluidic reaction chamber on the assembly formation. Fig. S2 shows formation of silanol layer during pre-activation of particles and their effect on robust assembly formation. Fig. S3 shows a comparison of our method to existing droplet methods.]

See DOI: 10.1039/c000000x/

References

1. Velev, O. D., Lenhoff, A. M., and Kaler, E. W., *Science*, 2000, **287**, 2240-2243
2. Dinsmore, A. D., Hsu, M. F., Nikolaides, M. G., Marquez, M., Bausch, A. R., and Weitz, D. A., *Science*, 2002, **298**, 1006-1009
3. Manoharan, V. N., Imhof, A., Thorne, J. D., and Pine, D. J., *Advanced Materials*, 2001, **13**, 447-450
4. Norris, D. J., *Nature Materials*, 2007, **6**, 177-178
5. Hara, Y., Mukaiyama, T., Takeda, K., and Kuwata-Gonokami, M., *Optics Letters*, 2003, **28**, 2437-2439
6. Hynninen, A. P., Thijssen, J. H. J., Vermolen, E. C. M., Dijkstra, M., and Van Blaaderen, A., *Nature Materials*, 2007, **6**, 202-205
7. Cho, A., *Science*, 2003, **299**, 1684-1685
8. Rolison, D. R., *Science*, 2003, **299**, 1698-1701
9. Rastogi, Vinayak and Velev, Orlin D., *Biomicrofluidics*, 2007, **1**, 014107-17
10. Burkert, K., Neumann, T., Wang, J. J., Jonas, U., Knoll, W., and Otteleben, H., *Langmuir*, 2007, **23**, 3478-3484
11. Hu, J., Zhao, X. W., Zhao, Y. J., Li, J., Xu, W. Y., Wen, Z. Y., Xu, M., and Gu, Z. Z., *Journal of Materials Chemistry*, 2009, **19**, 5730-5736
12. Liu, L., Li, P. S., and Asher, S. A., *Nature*, 1999, **397**, 141-144
13. Kim, S. H., Cho, Y. S., Jeon, S. J., Eun, T. H., Yi, G. R., and Yang, S. M., *Advanced Materials*, 2008, **20**, 3268+
14. Yi, G. R., Manoharan, V. N., Michel, E., Elsesser, M. T., Yang, S. M., and Pine, D. J., *Advanced Materials*, 2004, **16**, 1204+
15. Kim, J., Lee, J. E., Lee, J., Jang, Y., Kim, S. W., An, K., Yu, H. H., and Hyeon, T., *Angewandte Chemie-International Edition*, 2006, **45**, 4789-4793
16. Manoharan, V. N., *Solid State Communications*, 2006, **139**, 557-561
17. Takeoka, Y., Yoshioka, S., Teshima, M., Takano, A., Harun-Ur-Rashid, M., and Seki, T., *Scientific Reports*, 2013, **3**,
18. Wacker, J. B., Parashar, V. K., and Gijs, M. A. M., *Langmuir*, 2011, **27**, 4380-4385
19. Piret, F. and Su, B. L., *Chemical Physics Letters*, 2008, **457**, 376-380



A microfluidic process for on-chip formation of assemblies of oxide nanoparticles
68x40mm (300 x 300 DPI)